

# Development of microelectrodes for electrochemical micromachining

Yong Liu · Di Zhu · Yongbin Zeng · Hongbing Yu

Received: 25 May 2010 / Accepted: 9 November 2010 / Published online: 25 November 2010  
© Springer-Verlag London Limited 2010

**Abstract** Electrochemical micromachining (EMM) has become more and more important in micro machining in recent years. Microelectrode as the tool of EMM is an essential cell in the machining process. In this study, microelectrodes with various end shapes are fabricated by different processing techniques. First, the different end shape forming methods for microelectrode, such as electrochemical etching, single electric discharge, and electrochemical micromachining are investigated. Second, microelectrodes with various end shapes fabricated above are simulated, analyzed, and then used in EMM process. At last, micro holes array with diameter of less than 10  $\mu\text{m}$ , three micro holes with no taper and a 3D microstructure are machined on metallic materials by above three types of microelectrodes.

**Keywords** Electrochemical micromachining · End shape · Electrochemical etching · Single electric discharge · Micro holes · 3D microstructure

## 1 Introduction

With the development of Microelectromechanical System (MEMS), micromachining techniques have become a hot issue in modern industry. Micro-scale metal structures have a wide range of application in many fields, such as

biomedicine and aviation. As so far, micromachining techniques [1, 2] include: lithography, electrodischarge machining (EDM), ultrasonic machining, and electrochemical machining, etc. Electrochemical micromachining (EMM) is an electrochemical dissolution process that has many advantages, such as no tool wear, stress-free, and smooth surfaces, regardless of workpiece material hardness, strength, and high tension. As so far, many research attempts on electrochemical micromachining have been done [3–9]. It is proven that electrochemical micromachining is an effectual method to meet the needs of micro parts fabrication.

As tools of EMM and micro-EDM, the requirement of microelectrodes has been greatly increasing. Experiments show that the microelectrodes with different end shapes can be used for different purposes in the micromachining process [7–10]. In general, microelectrodes with diameter less than 50  $\mu\text{m}$  are often difficult to fabricate by conventional mechanical methods because it is easily bent by the lateral force [11, 12]. Wire electrodischarge grinding (WEDG) [13] is one of the proposed methods to overcome such limitation but low productivity is a very critical disadvantage. So, efficient methods for fabricating microelectrodes with different end shapes are needed now.

In this paper, the methods of fabricating microelectrodes with different end shapes are introduced firstly. Then, the different microelectrodes fabricated above are simulated and analyzed in EMM process. After that, the microelectrodes are used in EMM to verify their respective advantages. During the experiments, micro holes array with diameter of about 10  $\mu\text{m}$ , three micro holes with no taper, and a 3D microstructure are machined on metallic materials.

Y. Liu (✉) · D. Zhu · Y. Zeng · H. Yu  
College of Mechanical and Electrical Engineering,  
Nanjing University of Aeronautics and Astronautics,  
Nanjing 210016, China  
e-mail: rzliuyong@163.com

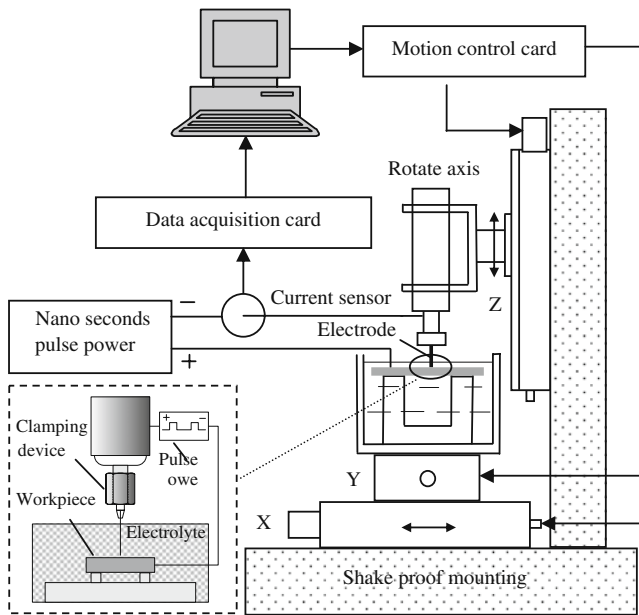


Fig. 1 Sketch of experimental system

2 Principle of EMM and experimental system

2.1 Principle of EMM

EMM is similar to common ECM which is an electrochemical anodic dissolution process. During the machining process, a short-pulse direct current with low voltage is passed between the workpiece and cathode. The anodic metal is dissolved into metallic ions by the electrochemical reaction. The micron scale cylindrical tungsten electrode is used as the cathode tool,

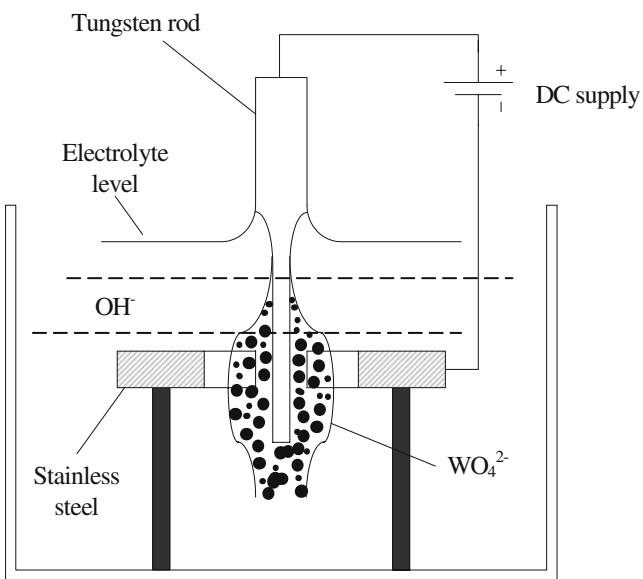


Fig. 2 Schematic diagram of fabricating microelectrode

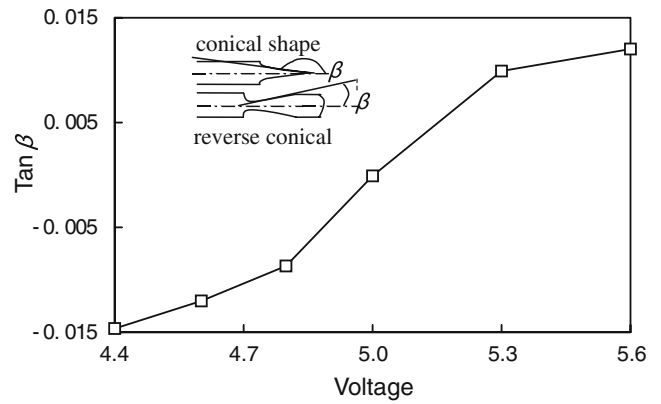


Fig. 3 Shape variation with applied voltage

and following the scheduled tool path, the required shapes or structures can be obtained. Dilute acid electrolyte, in which no sludge will be produced, can be used to improve the processing conditions.

2.2 Experimental system

In order to meet the EMM and micro electrical discharge machining experiments below, an experimental system with high-precision is set up. The developed experimental system consists of various sub-components, e.g., electrodes unit, controlled electrolyte flow system, servo-control feed unit, data acquisition system, and etc. Figure 1 presents a schematic view of the various system components of the developed experimental system. The electrodes unit consists of the tungsten rod, workpiece, tool holder, and electricity-conductive device. The controlled electrolyte flow system consists of the machining chamber, micro-meteor pump, filter, electrolyte tank, and so on.

The motion control system consists of a precise XYZ stage and servo-control feed unit. The motion parts of X, Y and Z axes are driven by direct-current servo motors with the resolution of 0.1  $\mu\text{m}$ . So, the experimental system is satisfied to machining micron-sized structures.

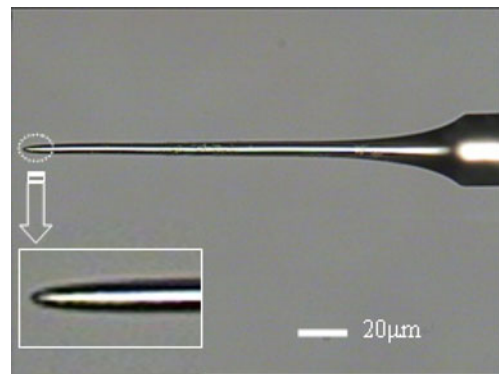


Fig. 4 A cylindrical electrode with diameter of 5  $\mu\text{m}$

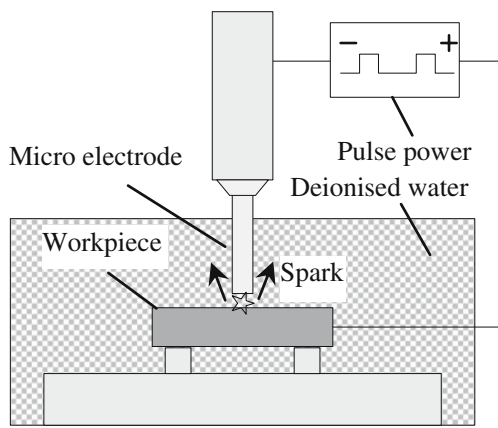


Fig. 5 Schematic diagram of single electrical discharge

During the EMM process, the stability is most important in which the machining gap is of several micrometers. If the tool feed rate is too high, the tool will come in contact with the workpiece and cause short circuit. By-product in the electrolyte may also cause short circuit to lead to the spark discharge. Since short circuiting seriously damages both the micro tool and the workpiece, a safety system is necessarily built in the setup. If the abnormal current signals are detected, the control system will rapidly change the velocity and the direction of the tool movement. For example, when a short circuit is detected, the servo motor will stop and move backward along the preceding path immediately until the danger is clear.

### 3 Fabrication of micro-electrodes with different end shapes

Lim et al. [14, 15] used KOH solution as electrolyte and direct current to fabricate the micro pins. The effects of

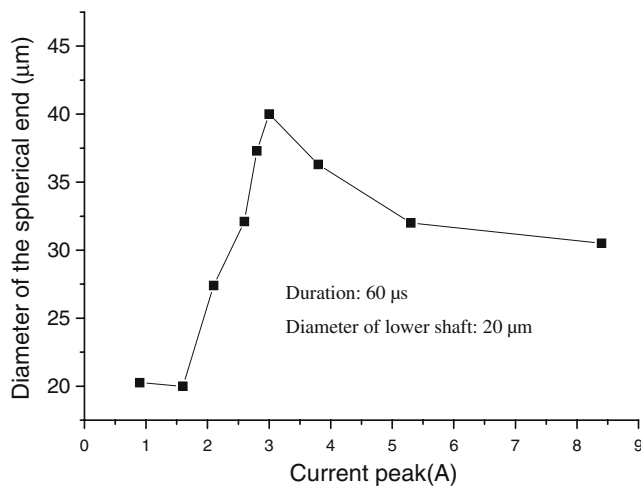


Fig. 6 Relations of spherical diameter and current peak

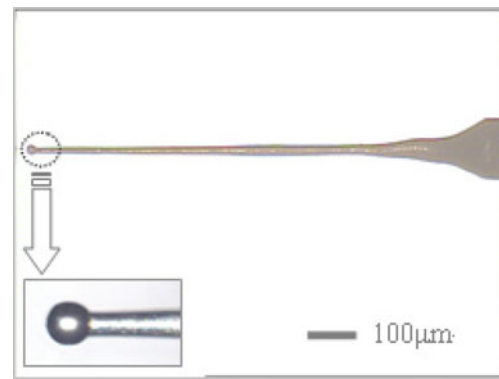
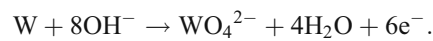


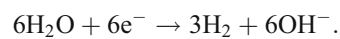
Fig. 7 A spherical end

current and voltage on the appearance of pins were discussed, and an appropriate current density which can produce cylindrical micro-pins was suggested. Based on the above theoretical mode, the etching cell for fabricating microelectrode in this study is shown in Fig. 2.

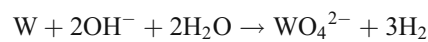
A straight tungsten rod as an initial electrode linked to the anode of power supply was located in the center of a stainless barrel. The stainless barrel was a cathode for rod etching. The rod immersed in NaOH solution at room temperature. When the machining voltage was applied, electrochemical reactions occurred between the electrodes. The anode tungsten dissolves by the following electrochemical reactions:



The electrochemical reaction on the cathode is:



And the overall reaction thus becomes



Experiments reveal that the electrode geometry is largely affected by the machining voltage. According to theory of

Table 1 Experimental conditions for fabricating spherical end

|                             |                 |
|-----------------------------|-----------------|
| Peak voltage, V             | 6               |
| Pulse on time, µs           | 60              |
| Pulse period, ms            | 1               |
| Cathode tool material       | WC              |
| Dielectric                  | Deionised water |
| Electrolyte temperature, °C | 26              |

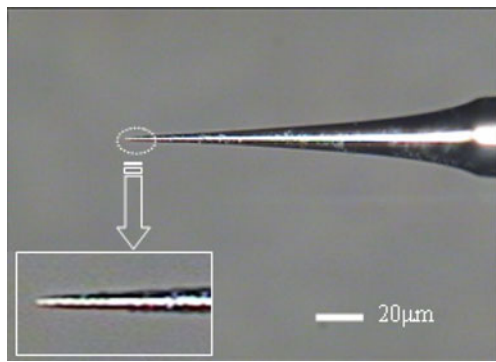


**Fig. 8** A conical end with tip diameter of less than 1  $\mu\text{m}$ . **a** Touch detection; **b** upward, rightward, and downward movement; **c** touch detection; **d** machining process; **e** finish

diffusion layer, high current density forms a thicker diffusion layer surrounding the tungsten electrode, which slows down the dissolved speed of the metal, and then, the tungsten electrode will become a reverse conical shape gradually. Otherwise, lower current density can produce a microelectrode with conical shape. So, in order to form a cylindrical electrode, the proper machining voltage has to be selected.

A set of experiments are carried out to seek the relationship between the taper  $\beta$  and the voltage. Here, the taper  $\beta$  is the angle between the surface and axis of the electrode. When the electrode is of conical shape, the angle  $\beta$  is an obtuse angle. While the electrode is of reverse conical shape, the angle  $\beta$  is an acute angle. Figure 3 shows the relationship between the  $\tan(\beta)$  value and the machining voltage. It proves that the  $\tan(\beta)$  value increases with voltage increase.

Machining conditions of the electrochemical etching process were as follows: initial electrode diameter of 300  $\mu\text{m}$ , 2 Mol/L NaOH electrolyte, and immersion depth of 2 mm. It is found that the proper voltage is around 5 V to fabricate the cylindrical electrode under the above processing conditions. As shown in Fig. 4, a cylindrical electrode with diameter of 5  $\mu\text{m}$  and length of 200  $\mu\text{m}$  was fabricated. As can be seen in the figure, the whole shape is quite inerratic and the etching time of the electrode is about 20 min.

**Table 2** Experimental conditions for fabricating conical end

|   |                       |
|---|-----------------------|
| Machining voltage, V                        | 4                     |
| Cathode tool material                       | Stainless steel       |
| Electrolyte                                 | 2 mol/L NaOH solution |
| Electrolyte temperature, $^{\circ}\text{C}$ | 26                    |
| Machining time, s                           | 30                    |

Although the whole shape of the above microelectrode is quite inerratic, the end shape of the electrode is not a regular cylinder. During the EMM process, the end shape of the microelectrode is easily copied to the workpiece. So, the end shape of the micro-electrode is a key point to keep the shape precision and machining accuracy of the workpiece. In order to obtain an inerratic end shape, the microelectrode in Fig. 4 needs secondary processing.

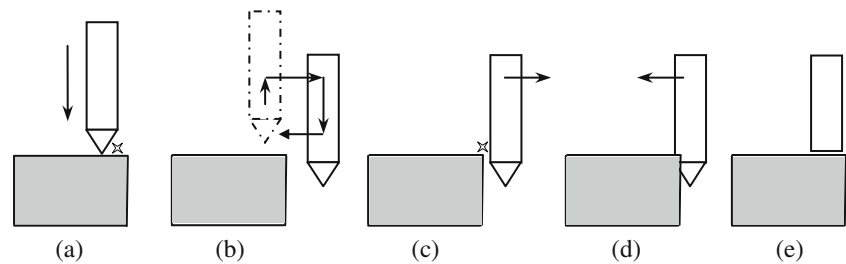
This paper presents the methods of processing spherical, conical, and flat end shapes on micro cylindrical electrode. And then, the related applications of the above electrodes in electrochemical micromachining are simulated and then verified by experiments.

### 3.1 Spherical end shape

The spherical end of the microelectrode is instantaneously fabricated by single electrical discharge in this paper. Figure 5 shows the schematic diagram of single electrical discharge. The basic process in EDM is carried out by producing controlled electric pulse sparks between the microelectrode and the workpiece, both of which are immersed in a dielectric fluid. The electric spark raises the surface temperature of both the electrode and the workpiece to a point where the surface temperatures exceed the melting or even boiling points of the substances. Then, metal of workpiece is thus primarily removed in the liquid and vapor states, and the micro-electrode wears at the same time. The greater the energy of a single discharge, the more of the substance is removed in a discharge. As a result, the wear of the electrode is much greater.

When the machining is carried out in deionised water at room temperature, the molten tungsten liquid becomes frozen immediately due to the great cooling capacity of deionized water. As a result, there is a sphere formed on the top of the tungsten electrode under the surface tension of liquid.

Experiments reveal that the diameter of spherical end is largely affected by the peak current. A set of experiments are carried out to seek the relations between the diameter of spherical end and the peak current. The relations between the diameter and peak current are as shown in Fig. 6. The diameter of the spherical end becomes larger when the peak current increases in the range of 0–3 A. But, the diameter of the spherical end becomes smaller when the peak current continues to increase. So, the suggested peak current is about 3 A. Figure 7 shows a spherical end diameter of about 40  $\mu\text{m}$  fabricated by current peak of 3 A. Table 1 shows the machining conditions of fabricating the spherical end.

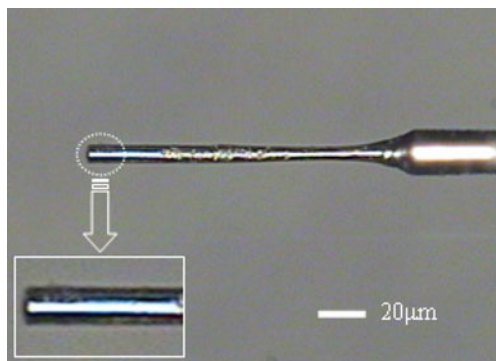
**Fig. 9** Machining procedure of cutting the tip off

### 3.2 Conical end shape

The conical end of microelectrode is fabricated by electrochemical etching process in this paper. According to the theory of diffusion layer, lower machining voltage can fabricate a sharp shape. So, in order to produce a conical end, the electrode is lifted and only remained the end part of microelectrode below the liquid level. Then, a lower voltage is shifted between the anode and cathode. A very sharp conical end can be obtained by controlling the machining time. Figure 8 shows a conical end with tip diameter of less than  $1\ \mu\text{m}$  and length of  $200\ \mu\text{m}$ . Table 2 shows the machining conditions of fabricating a conical end.

### 3.3 Flat end shape

The cylindrical electrode with flat end can be fabricated by WEDG or reverse EDM, but the above methods have some insurmountable disadvantages, such as low productivity and limitation of electrode size. So, the end tip of the cylindrical electrode in Fig. 4 is cut off to plane by electrochemical micromachining in this study. The machining procedure of cutting off the tip is shown in Fig. 9. First, the circumference of the electrode is detected with the contact detection function of the machining system. Second, the electrode is

**Fig. 10** A flat-tip electrode with diameter of  $6\ \mu\text{m}$ 

lifted and fed down to ensure the end tip of electrode under the upper surface of the cathode. Finally, the electrode is fed leftward to finish. As shown in Fig. 10, a flat-tip electrode with diameter of  $6\ \mu\text{m}$  and length of  $200\ \mu\text{m}$  was fabricated. Table 3 shows the machining conditions of fabricating a flat end.

## 4 Analysis about electric field and current density

For the purpose of discussing the applications of the above three types of microelectrodes in EMM process, the electric field analysis model is established to give a more realistic analysis of the current density distribution under the bottom and along the sidewall of the electrodes during the processing time.

According to Faraday's Law, the metal removal rate is depending on current density distributed on the workpiece surface during EMM [16]. In order to distinguish the different uses among the three types of electrodes, analysis about electric field and current density is carried out. Taking the electrode with plane working end for example, modeling and simulation in the gap have been done to observe the electric field and the current density distribution obviously as shown in Fig. 11. With some conditions and assumptions as follows:

1. The process of EMM is in the state of equilibrium;
2. The electrical parameters do not change with the time;
3. The conductivity and temperature of electrolyte are uniform.

**Table 3** Experimental conditions for fabricating flat end

|   |                         |
|---|-------------------------|
| Machining voltage, V                        | 4.5                     |
| Pulse on time, ns                           | 100                     |
| Pulse period, $\mu\text{s}$                 | 1                       |
| Cathode tool material                       | Stainless steel         |
| Electrolyte                                 | 0.1 mol/L NaOH solution |
| Electrolyte temperature, $^{\circ}\text{C}$ | 26                      |
| Feed speed, $\mu\text{m/s}$                 | 0.4                     |

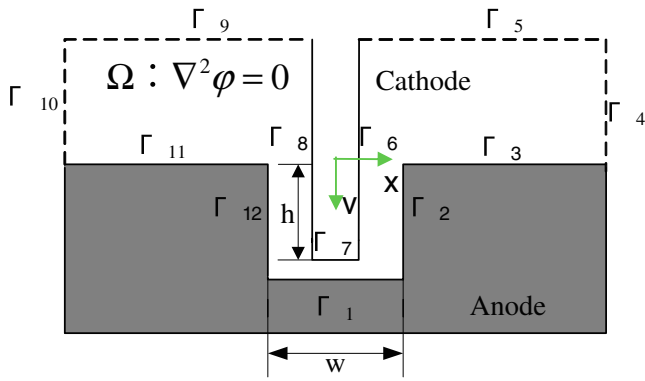


Fig. 11 Electric potential distribution in the interelectrode gap

The electric potential  $\phi$  in the interelectrode gap can be approximately described by Laplace's equation:

$$\Omega : \nabla^2 \phi = 0 \tag{1}$$

Boundary conditions are as follows:

$$\phi|_{\Gamma_{6,7,8}} = 0V \quad (\text{at the cathode tool}) \tag{2}$$

$$\phi|_{\Gamma_{1,2,3,11,12}} = U \quad (\text{at the anode surface}) \tag{3}$$

$$\frac{\partial \phi}{\partial n} |_{\Gamma_{4,5,9,10}} = 0 \quad (\text{the boundary condition}) \tag{4}$$

By using finite element method (FEM), the current density over the workpiece surface exposed in the electrolyte has been carried out in MEMS module of COMSOL Multiphysics with the scale:  $w=30 \mu\text{m}$ ,  $h=20 \mu\text{m}$ . Figure 12 shows the different current density distribution on the

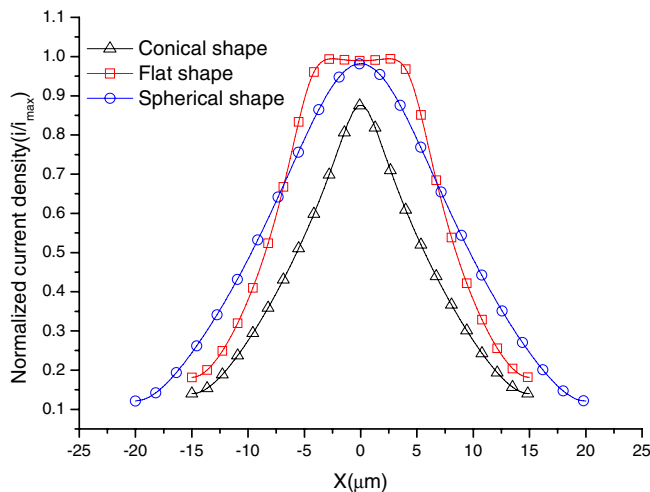


Fig. 12 Current density distribution over the underside surface of workpiece

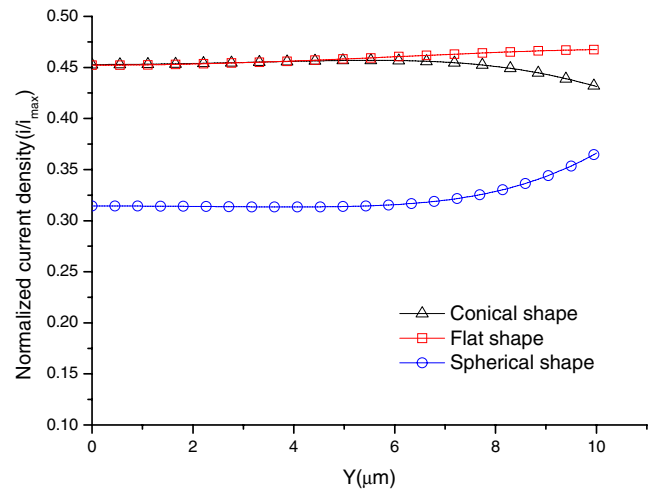


Fig. 13 Current density distribution along the sidewall surface of workpiece where  $x=\pm w/2$

underside surface of anode workpiece. As shown in Fig. 12, the current density distribution of the flat end is most well distributed, and the current density of the conical end is most concentrated and peaks at the center of the electrode and decreases rapidly from the center. Figure 13 shows the different current density distribution along the sidewall of anode workpiece, in which the  $y$  is the distance from the top surface to the position to be studied. As Fig. 13 has shown, the current density along the sidewall is reduced from about 46% to 31% by changing tool from the conical or flat end to the spherical end.

From what has been discussed above, it is proved that the cylindrical electrode with conical end can be used to fabricate very small micro holes due to its smaller diameter and the concentrated current density. The cylindrical electrode with flat end can be used to fabricate complex structures with planes due to its well-distributed current density. The cylindrical electrode with spherical end can be used to fabricate micro hole or structures with minor taper

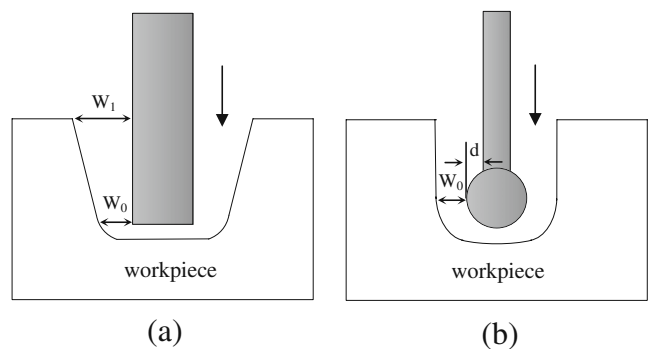
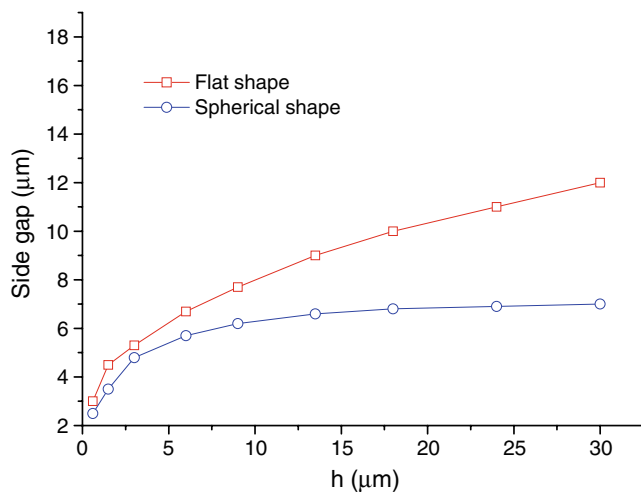


Fig. 14 Schematic of taper reduce





**Fig. 15** The change of side gap according to machining time

due to its smaller current density along the sidewall of the workpiece. For further research, the schematic of taper reduce is shown in Fig. 14. In EMM process, side gap increases with machining time. The increase in side gap causes the taper shape of structures. As Fig. 14a shows, the side gap increases with increase of machining depth when a cylindrical electrode with flat end is used. The initial side gap is  $w_0$ . However, it increases to  $w_1$  gradually during the machining process, then causes the taper shape around side wall. For machining of structures with no taper, a cylindrical electrode with spherical end is applied. Figure 14b shows the sketch of reducing taper shape when the spherical-tip electrode is used. For the micro spherical-tip electrode, the initial side gap is  $w_0 + d$  and makes the sidewall a lower current density, which avoids re electrolysis, and then the taper could be reduced.

To verify the effects of the spherical shape electrode on taper reduction, a set of contrast experiments were carried out. Thirty-micrometer-deep holes were machined on nickel plate respectively with  $\varnothing$  10- $\mu$ m flat-tip electrode and spherical-tip electrode. Figure 15 shows the different side gaps along the sidewall of anode workpiece, in which the  $h$  is the distance from the bottom surface to the holes entrance. It is proven that the side gap increases as the distance  $h$  increases. But, the side gaps of the spherical-tip

electrode increases less than the side gaps of the flat-tip electrode. With the time increasing, the side gaps of the spherical-tip electrode remain unchanged at about 7  $\mu$ m.

## 5 EMM using different electrodes

During the EMM processing, the nanosecond pulse voltage was applied between the electrodes to improve the machining location. Dilute sulfuric acid was preferred because the acid electrolyte usually produces much less by-product than common salt electrolytes, which is important for a steady machining process in so small machining gap. Table 4 shows the machining conditions for EMM.

### 5.1 Micro electrochemical drilling

For fabricating smaller micro hole, the cylindrical electrode with conical end was used. As shown in Fig. 16, the micro holes array which was machined using the tool with conical-tip diameter of less than 3  $\mu$ m at length of 20  $\mu$ m by EMM. The result shows a good repeatability, four holes with entry diameter of about 10  $\mu$ m were machined one by one on a 20- $\mu$ m-thick nickel plate. Pulses with 4.5 V and 45-ns pulse on-time were applied in 0.2 M  $H_2SO_4$ , and the feed rate was 0.1  $\mu$ m/s. Figure 15 also represents a local zoom of one hole, which has an entry diameter of 10  $\mu$ m and exit diameter of 7  $\mu$ m. The generated taper results from dissolution time difference between entry and exit together with tool electrode shape.

### 5.2 Taper reduce

To verify the taper reduce role of the spherical-tip electrode, three micro holes with diameter of about 80–100  $\mu$ m were machined by a  $\varnothing$  60  $\mu$ m spherical-tip electrode on a 0.8 mm thick nickelbase superalloy (GH3030) plate. Pulses with 4.5 V and 90–100 ns pulse on-time were applied in 0.2 M  $H_2SO_4$ , and the feed rate was 1  $\mu$ m/s. The cross-sectional view of holes is as shown in Fig. 17, the entry and exit diameters of the micro holes are almost the same. It is proved that the micro hole with negligible taper can be machined by the spherical-tip electrode.

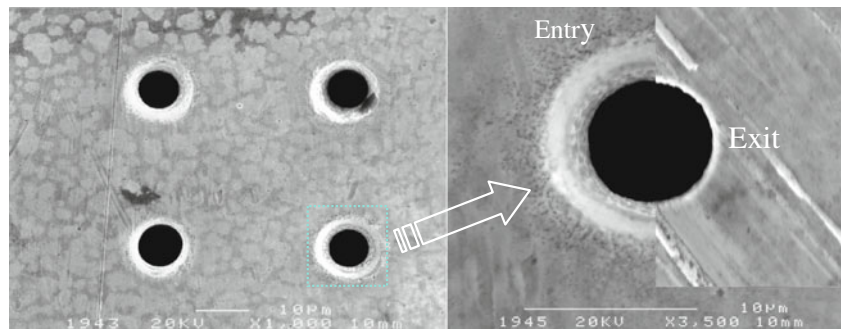
### 5.3 Milling of 3D structure with plane surfaces

For fabricating plane structures, the cylindrical electrode with flat end was used. Figure 18 shows a regular 3D structure with planes which was machined layer by layer using a flat-tip electrode with diameter of 10  $\mu$ m on a 300- $\mu$ m thick nickelbase superalloy (GH3030) plate. Pulses with 4.5 V and 90-ns pulse on-time were applied in 0.2 M  $H_2SO_4$ . As Fig. 18 shows, the size of selected plane domain is about

**Table 4** Experimental conditions for EMM

|                                      |                              |
|--------------------------------------|------------------------------|
| Machining voltage, V                 | 4.5                          |
| Pulse on time, ns                    | 45–100                       |
| Pulse period, $\mu$ s                | 1                            |
| Cathode tool material                | Ni/nickelbase superalloy     |
| Electrolyte                          | 0.2 mol/L $H_2SO_4$ solution |
| Electrolyte temperature, $^{\circ}C$ | 26                           |

**Fig. 16** Micro holes array with diameter of about 10  $\mu\text{m}$



55 $\times$ 25  $\mu\text{m}$ , and the micro column is of 5- $\mu\text{m}$  width, 55- $\mu\text{m}$  length and 30- $\mu\text{m}$  height. The SEM picture shows that EMM processing can achieve a good surface quality and machining precision by using the type of flat-tip electrode.

## 6 Conclusions

In this paper, microelectrodes with various end shapes are fabricated by different processing techniques. And then the

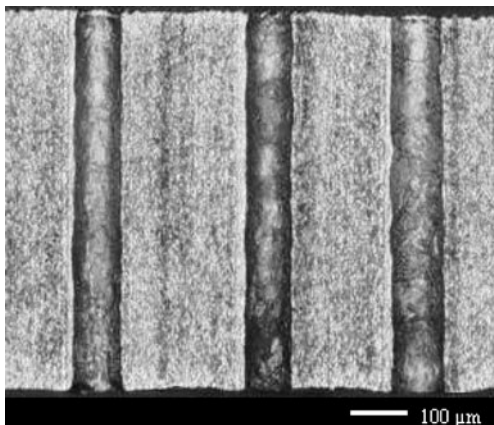
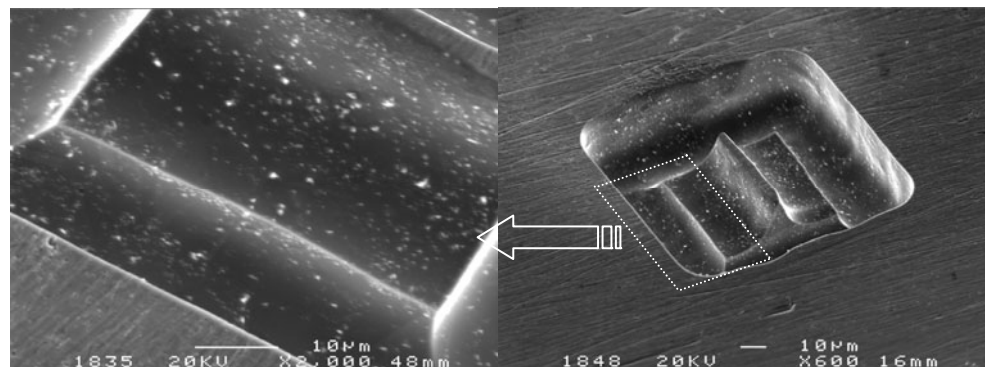


**Fig. 17** Micro holes with no taper

**Fig. 18** A 3D structure with plane surfaces



various electrodes are simulated and analyzed in EMM process. At last, groups of EMM experiments are carried out to verify the analysis results. The conclusions can be summarized as follows:

1. An experimental system for EMM with high-precision is established.
2. The spherical, conical, and flat-tip electrodes are fabricated respectively by single electric discharge, electrochemical etching process, and electrochemical micromachining technology.
3. Based on the results of simulation and analysis in EMM process, the conical-tip electrode should be used to fabricate much smaller micro holes, the flat-tip electrode should be used to fabricate complex plane structures layer by layer, and the spherical-tip electrode should be used to fabricate micro hole with no taper.
4. Finally, micro holes array with diameter of about 10  $\mu\text{m}$ , three micro holes with no taper, and a 3D structure with planes are successfully machined on metals. The experimental results prove that the analysis above is right, and also prove that electrochemical micromachining is a promising micromachining technique which can be used to process various micro parts.
5. For further research, microelectrodes with more other end shapes such as prism, spire, and so on, should be fabricated and used in the EMM process.



**Acknowledgements** This work was financially supported by the Chinese National Natural Science Funds (50635040), the National High-tech Research and Development Program (863 Program; 2009AA04Z302, 2009AA044205), and the Jiangsu Provincial Natural Science Foundation (BK2008043).

## References

- McGeough JA, Leu MC, Rajurkar KP, De Silva AKM, Liu Q (2001) Electroforming process and application to micro/macro manufacturing. *Ann CIRP* 50(2):499–514
- Rajurkar KP, Levy G, Malshe AP, Sundaram MM, McGeough JA, Hu X, Resnick R, DeSilva A (2006) Micro and nano machining by electro-physical and chemical processes. *Ann CIRP* 55(2):643–666
- Schuster R, Kirchner V, Allongue P, Ertl G (2000) Electrochemical micromachining. *Science* 289:98–101
- Trimmer AL, Hudson JL, Kock M, Schuster R (2003) Single-step electrochemical machining of complex nanostructures with ultrashort voltage pulses. *Appl Phys Lett* 82:3327–3329
- Bhattacharyya B, Munda J, Malapati M (2004) Advancement in electrochemical micro-machining. *Int J Mach Tools Manuf* 44(15):1577–1589
- Lee ES, Baek SY, Cho CR (2005) A study of the characteristics for electrochemical micromachining with ultrashort voltage pulses. *Int J Adv Manuf Technol* 31:762–769
- Kim BH, Ryu SH, Choi DK, Chu CN (2005) Micro electrochemical milling. *J Micromech Microeng* 15(1):124–129
- Kim BH, Na CW, Lee YS, Choi DK, Chu CN (2005) Micro electrochemical machining of 3D micro structure using dilute sulfuric acid. *Ann CIRP* 54(1):191–194
- Kurita T, Chikamori K, Kubota S, Hattori M (2006) A study of three-dimensional shape machining with an EC $\mu$ M system. *Int J Mach Tools Manuf* 46:1311–1318
- Ekvall I, Wahlström E, Claesson D (1999) Preparation and characterization of electrochemically etched W tips for STM. *Meas Sci Technol* 10(1):11–18
- Yamagata Y, Higuchi T (1995) Three-dimensional micro fabrication by precision cutting technique. *J Jpn Soc Precision Eng* 61(10):1361–1364
- Waida T, Okano K (1995) Micro-grinding of micro-machine component. *J Jpn Soc Precision Eng* 61(10):1365–1368
- Masuzawa T, Fujino M, Kobayashi K, Suzuki T, Kinoshita N (1985) Wire electro-discharge grinding for micro-machining. *Ann CIRP* 34(1):431–434
- Lim YM, Kim SH (2001) An electrochemical fabrication method for extremely thin cylindrical micropin. *Int J Mach Tools Manuf* 41(15):2287–2296
- Wang MH, Zhu D, Zhang ZY (2006) Fabrication of micro-pin based on electrochemical etching. *Chin J Mech Eng* 42(6):128–132
- Qian SQ, Zhu D, Qu NS, Li HS, Yan DS (2010) Generating micro-dimples arrays on the hard chrome-coated surface by modified through mask electrochemical micromachining. *Int J Adv Manuf Technol* 47:1121–1127